A Water-Soluble Polymer-Lumefantrine Conjugate for the Intravenous Treatment of Severe Malaria

*William M.R. Matshe, Lesego L. Tshweu, Sindisiwe Mvango, Zamani E.D. Cele, Avashnee S. Chetty, Lynne A. Pilcher, Ibukun M. Famuyide, Lyndy J. McGaw, Dale Taylor, Liezl Gibhard, Gregory S. Basarab, Mohammed O. Balogun**

W. M. R. Matshe, L. L. Tshweu, S. Mvango, Z. E. D. Cele, A. S. Chetty, M. O. Balogun

Bio-Polymer Modification and Therapeutics Laboratory, Centre for Nanostructures and Advanced Materials, CSIR, Pretoria, 0001, South Africa.

E-mail: *mohammedbalogun@tuks.co.za

S. Mvango, L. A. Pilcher

Department of Chemistry, University of Pretoria, Lynnwood Road, Hatfield, Pretoria, 0002, South Africa.

I. M. Famuyide, L. J. McGaw

Phytomedicine Programme, Department of Paraclinical Sciences, Faculty of Veterinary Science, University of Pretoria, Private Bag X04, Onderstepoort, Pretoria, 0110, South Africa.

D. Taylor, L. Gibhard, G. S. Basarab

Drug Discovery and Development Centre (H3D), Department of Chemistry, University of Cape Town, Rondebosch, Cape Town, South Africa.

This article has been accepted for publication and undergone full peer review but has not been through the copyediting, typesetting, pagination and proofreading process, which may lead to differences between this version and the Version of Record. Please cite this article as doi: 10.1002/mabi.202200518.

Keywords: Severe malaria, artemisinin-based combination therapy, lumefantrine, polymer therapeutics, drug delivery, nanomedicine, infectious disease.

Highlights

- A water-soluble polymer therapeutic nanomedicine of lumefantrine was prepared.
- The polymer-lumefantrine conjugate was administered intravenously in a clinically relevant aqueous formulation.
- Significant antiplasmodial activity was demonstrated for the first time in a *Plasmodium falciparum*-infected mouse model.

Abstract

Uncomplicated malaria is effectively treated with oral artemisinin-based combination therapy (ACT). Yet, there is an unmet clinical need for the intravenous treatment of the more fatal severe malaria. There is no combination intravenous therapy for this form of the disease mainly due to the nonavailability of a water-soluble partner drug for the artemisinin, artesunate. The currently available treatment is a two-part regimen split into an intravenous monotherapy artesunate administered while the patient is admitted to a health centre and followed by the conventional oral ACT that is taken after the patient has been discharged. In a novel application of polymer therapeutics, we conjugated the aqueous insoluble but very important antimalarial lumefantrine to a carrier polymer to create a new water-soluble chemical entity (p-*N*-acryloylmorpholine-stat-p-acrylic acid-Lumefantrine) suitable for intravenous administration in a clinically relevant formulation. The conjugate is characterized by spectroscopic and analytical techniques, and the aqueous solubility of lumefantrine is determined to have increased by about three orders of magnitude. Pharmacokinetic studies in mice indicates that there is significant release of lumefantrine in the plasma at relatively high concentrations and production of the liver metabolite desbutyl-lumefantrine (area under the curve of metabolite is about 10% that of the parent). In a *Plasmodium falciparum* severe malaria mouse model, parasitaemia clearance by PNAM-Lumefantrine is 50% higher than that of reference unconjugated lumefantrine. The polymer-lumefantrine shows potential for

entering the clinic as a partner drug to artesunate to meet the need for a one-course treatment for severe malaria.

Graphical abstract

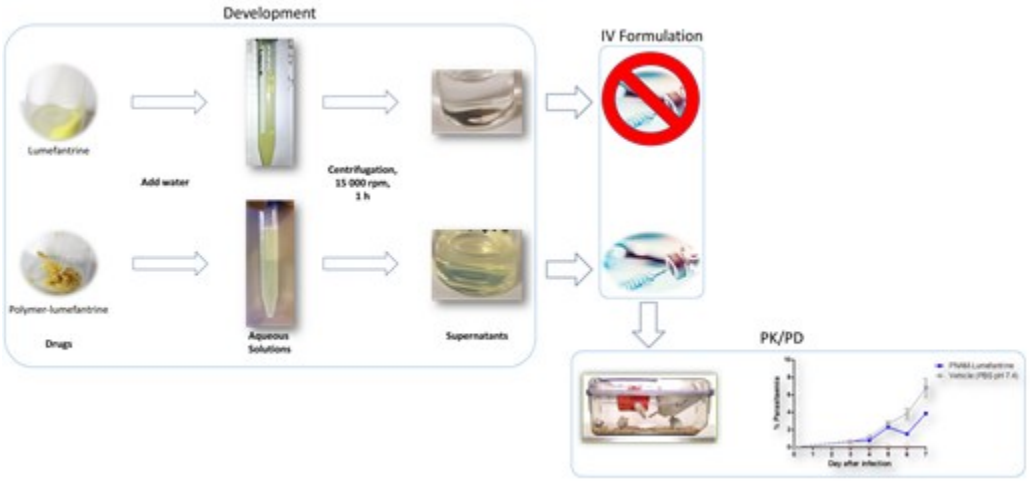

The aqueous solubility of the major antimalarial lumefantrine is increased over x10^3 by conjugation to a carrier polymer in a novel application of polymer therapeutics nanomedicine technology. The polymer-drug conjugate is successfully demonstrated as suitable for the intravenous treatment of severe *Plasmodium falciparum* malaria in preclinical trials in mice.

1. Introduction

Malaria is an ancient infectious disease that is still one of the deadliest today. Although it has been eliminated in about 40 countries—the most notable recent one being China—success against the disease has been mixed and uneven. Myanmar, Laos, Vietnam (three countries that share borders with China) and much of the African continent remain malaria endemic. With 95% of global malaria cases, Sub-Sahara African countries continue to bear a

disproportionate burden of the disease (1). Nigeria alone accounts for about 27% of global infections and along with five other African countries, accounted for just over half of deaths in 2020.

Malaria is caused by the protozoan *Plasmodium* spp. Of the six species that infect humans, *P. falciparum* is responsible for over 99% of cases in Africa and more than 50% of cases in other malaria-endemic regions. *P. falciparum* infection can progress to severe or complicated malaria, which presents distinct symptoms that include cerebral malaria, renal and other organ failures, pulmonary oedema, hypoglycaemia, severe anaemia, and acidosis that often lead rapidly to unconsciousness and death if not managed adequately (2,3).

Severe malaria is treated with a two-part regimen. Firstly, an intravenous course of artesunate (a water-soluble artemisinin derivative) is administered for 24 hours or until it is safe to take substances orally (4,5). The second part of the treatment is an oral artemisinin-based combination therapy (ACT). The use of a monotherapy that effectively alleviates the serious clinical symptoms of patients could ironically increase the risk of non-compliance with the additional full three-day course of ACT (6). This would expose the artemisinins to a higher risk of drug resistance from the malaria parasites (7–9). One strategy to minimize this risk and ensure treatment completion would be to administer an intravenous ACT treatment from the outset that could render the follow-up oral course unnecessary. Intravenous ACT treatment would require a water-soluble partner drug to combine with artesunate.

Lumefantrine belongs to the class of antimalarials known as arylamino alcohols. First synthesized by the Chinese military in the 1970s, it was registered for the treatment of malaria in 1987. It has only been administered orally in combination with an artemisinin-based drug. Its main role is to clear residual or slow-maturing parasites that might have evaded the faster-acting artemisinin. Lumefantrine has been found to attenuate resistance to the artemisinins and demonstrates synergistic activity with artemether in particular (10). Combination of lumefantrine with artesunate in a single intravenous treatment for severe malaria would serve as a strategic bulwark against the increasing risk of resistance to the entire ACT. However, with the low aqueous solubility of 3.0×10^{-5} mg/ml for lumefantrine, this has not been an option. An attempt to develop an intravenous formulation of lumefantrine was reported by Prabhu et al. (11). Although the increase in aqueous solubility achieved was not reported, the combination was used in the treatment of a murine model of

severe malaria where the animals were infected with the non-human *P. berghei* parasite. NLCs are particulate lipid encapsulation of hydrophobic drugs that are solubilized by an interfacial corona of surfactants. Polymorphic changes in the lipid core can cause premature release of the entrapped drug (12). Encapsulated nanoparticles are also known to experience challenges with stability during storage and *in vivo* performance, the latter presumably due to slow release/low free fraction of drug (13–16).

Conjugation of hydrophobic drugs to water-soluble polymers is used to increase solubility and improve pharmacokinetics (17,18). Many of the major anticancer drugs like camptothecin, paclitaxel, and doxorubicin have been conjugated to hydrophilic polymers and have seen their solubilities increased such that they can be administered as aqueous formulations (19–21). The application of polymer-drug conjugation in malaria chemotherapy has however been limited to a few drugs like dihydroartemisinin (DHA) and primaquine (22,23). Polymer-DHA conjugates have mostly been investigated as potential anticancer therapeutics rather than as antimalarials. Recently, a polymeric prodrug of lumefantrine was synthesized and used to encapsulate artemether in an unsuccessful attempt to demonstrate a potential ACT nanomedicine (24). There was also no indication of the degree of aqueous solubility achieved from conjugating lumefantrine to the water-soluble block copolymer of poly(N-vinylpyrrolidone) and poly(α-allylvalerolactone), and the nanoaggregate combination showed no antiplasmodial activity *in vitro*, which was attributed to slow aggregate disassembly. We report the development of a polymer-lumefantrine conjugate and demonstrate its therapeutic potential by intravenous administration in a clinically relevant aqueous formulation to mice infected with the *P. falciparum* human parasite.

2. Materials and Methods

Lumefantrine (99%) was purchased from DB Fine Chemicals Pty Ltd (South Africa). Dimethylformamide (DMF, anhydrous 99.8%), dimethylaminopyridine (DMAP, >99%), diisopropylethylamine (DIEA, >99%), diisopropylcarbodiimide (DIC, >99%), hydroxybenzotriazole (HOBt, >97%), dichloromethane (DCM, ACS grade, >99%), acetonitrile (ACN, HPLC grade, >99%), acetone (>90%), methanol (MeOH, HPLC grade, >98%), formic acid (HPLC grade, >98%) were all purchased from either Sigma-Aldrich Ltd

(South Africa) or CRD Chemicals Pty Ltd (South Africa). All other reagents and solvents, unless otherwise stated, were purchased from Sigma-Aldrich Ltd (South Africa). Gases were purchased from Afrox and Air Products, South Africa. Phosphate buffer and phosphate-buffered normal saline were used at pH 7.4.

p-*N*-acryloylmorpholine-stat-p-acrylic acid (PNAM; Mn = 17 KDa, Đ = 1.13, DP = 100) was received as a generous donation from Dr Joaquin Sanchis and Ms Sun Cheng of Monash Australia. Its molar mass distribution curve is presented in the Supplementary data **Figure S1**.

The proton nuclear magnetic resonance (^{1}H NMR) spectra were acquired on a Bruker 400 AVANCE Ultrashield+ instrument (Bruker, United Kingdom) at 295.4 K, with test samples prepared in deuterated chloroform ($CDCl_3$). The data were processed with Mestrenova software version 6.2.2-5475. Fourier Transform Infrared spectroscopy (FT-IR) spectra were acquired on Perkin Elmer Spectrum 100 (USA) within a range of 650-4000 cm^{-1} with four scans performed for each sample at a resolution of 4 cm^{-1}. Ultraviolet/visible light (UV/Vis) absorptions were measured on a Mettler Toledo UV5Bio UV/Vis spectrophotometer (Mettler Toledo, USA). Malvern Zetasizer Nano-ZS90 (Malvern Instruments, United Kingdom) was used to determine the hydrodynamic size and zeta potential.

2.1. Chemistry

2.1.1. Synthesis of PNAM-Lumefantrine conjugate

To a stirring solution of PNAM (200 mg, 0.015 mmol) in anhydrous DMF (5 ml) was added DIC (58.23 mg, 0.46 mmol), HOBt (62.34 mg, 0.46 mmol) and DMAP (0.01 mmol). The reaction mixture was basified with DIEA, lumefantrine (16.30 mg, 0.031 mmol) added and left to stir under N_2 gas at 35 °C in the dark. After 48 h, the reaction was stopped with the removal of DMF *in vacuo* at 5 mBar. Phosphate buffer (10 ml) was added to the crude slurry and left to stir for 1 h at 35 °C. The suspension was centrifuged at 21 000 *x g* for 1 h at 5 °C and the supernatant withdrawn, dialyzed in phosphate buffer with a PUR-A-LYZER membrane dialysis kit (MWCO: 1 kDa) at room temperature (20 °C – 25 °C) for 72 h with three changes of the buffer. The pure PNAM-Lumefantrine conjugate was obtained as a yellowish powder after lyophilisation.

2.2. *In vitro* Assays

2.2.1. *In vitro pLDH antiplasmodial assessments*

The IC_{50} of the PNAM-Lumefantrine conjugate was determined using 3D7 strain of *P. falciparum* in an established enzymatic assay that involves the parasite lactate dehydrogenase (pLDH), which is distinguishable from the host's enzyme (25). Lactate dehydrogenase is an enzyme found in all cells, and it catalyzes the conversion of lactate to pyruvate with the reduction of the co-enzyme nicotinamide adenine dinucleotide (NAD) to NADH. In parasites, the NAD analogue APAD (3-acetylpyridine adenine nucleotide) is reduced to APADH and upon this reduction, the yellow NBT/PES (nitro blue tetrazolium + phenazine ethosulphate) is converted to purple formazan crystals. The formation of these crystals is indicative of the pLDH activity and the survival of parasites. Before conducting the assay, an assessment of parasitaemia levels of parasitized red blood cells (pRBCs) was conducted. Parasitaemia counts were done in areas within the vision grid of a microscope lens where RBCs were evenly spread on Giemsa-stained glass slides. The number of parasite-infected cells and total RBCs in the vision grid were respectively counted 10 times at random across the slide. The per cent (%) parasitaemia was determined with the formula:

$$\%Parasitaemia = \frac{RBCs\ infected\ with\ parasite}{9\ \times\ RBCs\ in\ small\ square}\ \times\ 100\%$$

Parasitaemia level was adjusted to 2% before the pLDH antiplasmodial assay. See Supplementary information for detailed protocol.

A stock solution of PNAM-Lumefantrine (20 mg/ml) was prepared in phosphate-buffered saline (PBS) solution. From this, ten serial dilutions of concentrations between 100 µg/ml - 5.13 x 10^{-3} µg/ml were prepared for the dose-response studies. The reference standards (chloroquine and artemisinin) were also prepared at 20 mg/ml and tested at 1000 ng/ml - 0.051 ng/ml dilutions. To each serially diluted test compound in a 96-well plate, 100 µl of 2% parasitaemia at 2% haematocrit suspension was added, except for the control wells. The plates were then placed in a container, gassed with a special gas mixture (90% N_2, 5% O_2 and 5% CO_2) for 2 min and incubated at 37 °C for 48 h. The absorbance was read at 620 nm on an Infinite F500 multiwell spectrophotometer (Tecan Group Ltd., Switzerland). The experiments were performed in triplicates for all samples.

2.2.2. *In vitro SYBR Green I antiplasmodial assessment*

In vitro antiplasmodial activity of the PNAM-Lumefantrine conjugate was conducted at the Malarial Parasite Molecular Laboratory of the University of Pretoria, South Africa. *P. falciparum* NF54 cultures were maintained at 37 °C in human erythrocytes (O^+/A^+) suspended in a complete culture medium (RPMI 1640 medium (Sigma-Aldrich) supplemented with 25 mM HEPES (Sigma-Aldrich), 20 mM D-glucose (Sigma-Aldrich), 200 µM hypoxanthine (Sigma-Aldrich), 0.2% sodium bicarbonate, 24 µg/ml Gentamicin (Sigma-Aldrich) and 0.5% AlbuMAX II) in a gaseous environment of 90% N_2, 5% O_2, and 5% CO_2 as previously described (26). *In vitro* ring-stage, intraerythrocytic *P. falciparum* cultures (genotyped drug sensitive strain, 200 µl at 1% haematocrit, 1% parasitaemia), were treated with PNAM-Lumefantrine, unconjugated lumefantrine, and PNAM. The controls for this assay included chloroquine diphosphate (1 µM, as positive control) and complete RPMI media (as negative control) and grown for 96 h at 37 °C under the 90% N_2, 5% O_2, and 5% CO_2 gas mixture in 96-well plates. At the conclusion of the 96-hour growth period, equal volumes (100 µl each) of the *P. falciparum* cultures were combined with SYBR Green I lysis buffer (0.2 µl/ml 10 000x SYBR Green I, Invitrogen; 20 mM Tris, pH 7.5; 5 mM EDTA; 0.008% (w/v) saponin; 0.08% (v/v) Triton X-100). The samples were incubated for 1 h at room temperature after which the fluorescence was measured using a GloMax-Explorer Detection System with Instinct Software (Promega, excitation at 485 nm and emission at 538 nm). The 'background' fluorescence (i.e., that measured in the samples derived from chloroquine-treated infected erythrocytes in which parasite proliferation was completely inhibited) was subtracted from the total fluorescence measured for each sample to provide a measure of parasite proliferation. The experiments were performed in technical triplicates for three biological repeats (n = 3). The data obtained were analysed in Microsoft Excel and the graphs plotted using GraphPad Prism 7 software (California, USA).

2.2.3. In vitro cytotoxicity assessment

The cytotoxicity of the PNAM-Lumefantrine was investigated in Vero (ATCC CCL-81) cells obtained from the kidneys of the African green monkey and in the human Caucasian colon adenocarcinoma (Caco-2, ATCC HTB 37) cell line. Vero cells were maintained in Minimum Essential Medium (MEM, Highveld Biological, South Africa) supplemented with 5% foetal calf serum (Adcock-Ingram, South Africa) and 0.1% gentamicin (Virbac, South Africa) in a 5% CO_2 incubator. The Caco-2 cells were grown in Dulbecco's Modified Eagle's Medium

(DMEM, Highveld Biological, South Africa) supplemented with 10% foetal calf serum (Adcock-Ingram), 1% non-essential amino acids (Hyclone, USA) and 1% penicillin-streptomycin (10,000 U/ml and 10 mg/ml streptomycin) in a 5% CO_2 incubator.

Cell suspensions were prepared from 70-80% confluent monolayer cultures and plated at a density of 5×10^4 cells into each well of sterile flat-bottom 96-well microtiter cell culture plates. Plates were incubated for 24 h at 37 °C in a 5% CO_2 incubator before exposure to the test compounds, which were dissolved in DMSO, appropriately diluted with the complete media to concentrations from 0.4 mg/ml to 0.005 mg/ml and added to the wells with further incubation for 48 h Doxorubicin (Pfizer, USA) and DMSO served as positive and negative controls, respectively. After the incubation period, the wells were rinsed twice with 200 µl of PBS and 200 µl of fresh medium was dispensed into the wells. Then 3-(4,5-dimethylthiazol-2-yl)-2,5-diphenyltetrazolium bromide (MTT, 30 µl, 5 mg/ml) dissolved in PBS was added to each well and the plates were further incubated for 4 h at 37 °C. After this, the medium from the wells was discarded and 50 µl of 100% DMSO was added to the wells to dissolve the formed formazan crystals. Absorbance was measured on a microplate reader (BioTek Synergy, USA) at a wavelength of 570 nm. Each compound was tested in quadruplicate and the assay was repeated twice. The equation resulting from a plot of the log of the concentration versus absorbance was used to calculate the concentration response for 50% lethality against the cells (LC_{50}).

2.3. *In vivo* Pre-Clinical Studies

The pharmacokinetics (PK) and pharmacodynamics (PD) (antimalarial efficacy) studies of the PNAM-Lumefantrine conjugate were carried out using healthy male Balb/c mice (PK only, three animals per group) and *P. falciparum*-infected NSG mice (PK and PD, two animals per group), respectively, maintained at the Pharmacology Satellite Animal Facility, Groote Schuur Hospital, Cape Town, South Africa. All the animals were housed in an air-conditioned facility (22 ± 3 °C; 40-70% relative humidity) with 20 air changes per hour and 12 h light/dark cycles. Cages were well-ventilated and contained autoclaved wood shavings. They were fed autoclaved pellets and sterile water *ad libitum*. Animals were weighed and the dosages of the test compounds were calculated a day before dosing.

2.3.1. *Pharmacokinetics*

Animal preparation

PNAM-Lumefantrine was dissolved in PBS to a drug concentration of 3.12% (w/v). Unconjugated lumefantrine reference was dissolved in dimethylacetamide (DMA) and made up with polyethylene glycol (PEG; Mol. wt. = 400 Da) and propylene glycol (PPG) in a volume ratio of 10: 30: 60 (DMA: PEG: PPG). Both solutions were prepared to deliver a 2.0 mg/kg dose of lumefantrine in 200 µl. The dosages were prepared 60 minutes prior to administration to the animals via the tail vein as a bolus under general anaesthetic (0.1 ml of ketamine (120 mg/kg)-xylizine (16 mg/kg) mixture per mouse) and sterilized by push filtration. Animal welfare was monitored throughout the exposure and sampling period as per approved protocols.

Sample collection

A whole-blood sampling of approximately 35 µl per animal was carried out via tail vein bleeding into heparinized tubes at pre-determined time points. For PK studies in healthy Balb/c mice, samples were collected at 0 h, 0.17 h, 0.5 h, 1 h, 3 h, 5 h, 7 h, 10 h, 24 h, and 48 h while in the *Plasmodium*-infected NSG mice, sampling was at 0 h, 0.17 h, 0.5 h, 1 h, 3 h, 5 h, 8 h, and 24 h after dosing. Samples for PK studies in infected mice were only collected for 24 h because dosing was repeated for three more days as per the efficacy studies protocol. Once drawn, samples were kept on ice until time points had been taken from all animals and transferred to a freezer for storage at -80 °C until extraction.

Sample preparation and LC-MS analysis

Frozen whole blood samples were thawed at room temperature and vortexed. For healthy mice, 30 µl of whole blood was mixed with three volumes of 100% ACN plus the internal standard, vortexed for 30 s and centrifuged. The supernatant was transferred to a borosilicate vial and dried at 30 °C under a constant flow of N_2 gas. Infected mouse sample preparation was done by an analogous protein precipitation and extraction method except that only 10 µl of whole blood and 100 µl ACN containing the internal standard were used. Calibration standards and quality controls were also subjected to the same extraction procedure.

The concentrations of lumefantrine and its major metabolite, desbutyl-lumefantrine, in the prepped samples were determined using a quantitative LC-MS/MS method. Samples were reconstituted in a mixture of the mobile phases (A/B: 3/7) and injected onto the column for LC-MS/MS analysis. The calibration standard and quality control standards were analysed in triplicates. LC-MS/MS analytical conditions are reported in Supplementary Information **Table S4**.

PK data analysis

The experimental data were evaluated as drug concentration versus time. A non-compartmental analysis was performed for the determination of the PK parameters using PK Solutions v2.0 (Summit Research Services, Montrose, USA). A quadratic regression, with peak area ratio (Drug/internal standard) against concentration with 1/concentration (1/x) weighting, was fitted to the calibration curves.

2.3.2. Antimalarial efficacy study

Animal preparation, infection with parasite and treatment dosing

The therapeutic efficacy of PNAM-Lumefantrine was evaluated using a '4-day test'. Briefly, four groups of NOD-*scid IL-2Rγ*^{null} mice, with two mice per group, were engrafted with human erythrocytes (approximately 60%) and infected with 2 x 10^7 *P. falciparum* Pf3D7$^{0087/N9}$-infected erythrocytes propagated from a donor mouse generated at GlaxoSmithKline, Tres Cantos (Spain) (27). Infections were initiated via intravenous injection of the parasite on Day 0 through the penile vein. Treatment through the tail vein with a single intravenous dose of the drug per day (100 µl per mouse) commenced on Day 3 and ended on Day 6 following infection. The PNAM-Lumefantrine conjugate formulated in PBS only and the unconjugated lumefantrine reference formulated in DMA: PEG: PPG (10: 30: 60) were administered at 1.0 mg/kg body weight. A vehicle-only group was also included as a negative control for the conjugate (PBS) and the unconjugated lumefantrine reference (DMA: PEG: PPG; 10: 30: 60). In all cases, parasitaemia was assessed by flow cytometry in samples of peripheral blood obtained on days 3, 4, 5, 6, and 7 after infection.

Sample analysis

The effect of treatment on the chloroquine-sensitive *P. falciparum* Pf3D7$^{0087/N9}$ was assessed by microscopy and flow cytometry. Fresh samples of peripheral blood from infected mice were stained with TER-119-PE (marker for murine erythrocytes) and SYTO-16 (nucleic acid dye) and then analysed via flow cytometry on a BD Accuri C6 Plus.

Efficacy data analysis

Data analysis used a non-linear fitting to logistic equation of $\log_{10}$ (% parasitaemia at Day 7 after infection) within GraphPad software.

3. Ethics

All *in vitro* and *in vivo* experiments and handling of animals were conducted under approved protocols granted by the CSIR Research Ethics Committee (*ref no.: 220/2017*) and the University of Cape Town's Faculty of Health Sciences Animal Ethics Committee (*ref no.: 014/028*).

4. Results

4.1. Synthesis of PNAM-Lumefantrine conjugate

Conjugation of lumefantrine to PNAM via an ester linker was successfully achieved in a one-pot reaction that involved the activation of the carboxyl groups of the polymer with DIC (**Figure 01**). To ensure maximum drug loading, excess molar equivalents of DIC and lumefantrine were used under an inert atmosphere and at a slightly raised temperature (35 °C) of the reaction mixture. The successful synthesis of the PNAM-Lumefantrine conjugate was confirmed by the downfield shift of the oxymethine proton to a broad peak at 5.55 ppm in the ^{1}H NMR spectrum of the purified product (**Figure 02**. **A**). Peak broadening is often attributable to interaction of the drug with the polymer. The drug loading was determined to be 12.2 mol% using protons marked 13-16 for the polymer and the aromatic (7.0 ppm) and methyl (0.7 ppm) proton peaks of the drug. The aromatic protons of lumefantrine are visible downfield as multiplets at σ 8.00-7.27. ATR-FTIR analysis showed an absorbance shift from 1723.7 cm^{-1} of the unconjugated polymer to 1699.5 cm^{-1} for the conjugate, which was attributed to the carbonyl of the ester bond (Supplementary Information **Figure S2**).

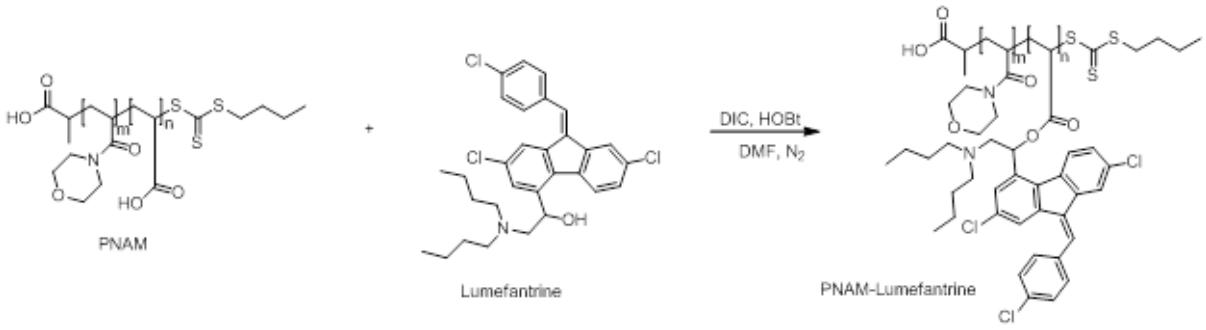

Figure 01. Synthesis of PNAM-Lumefantrine conjugate with an ester linker.

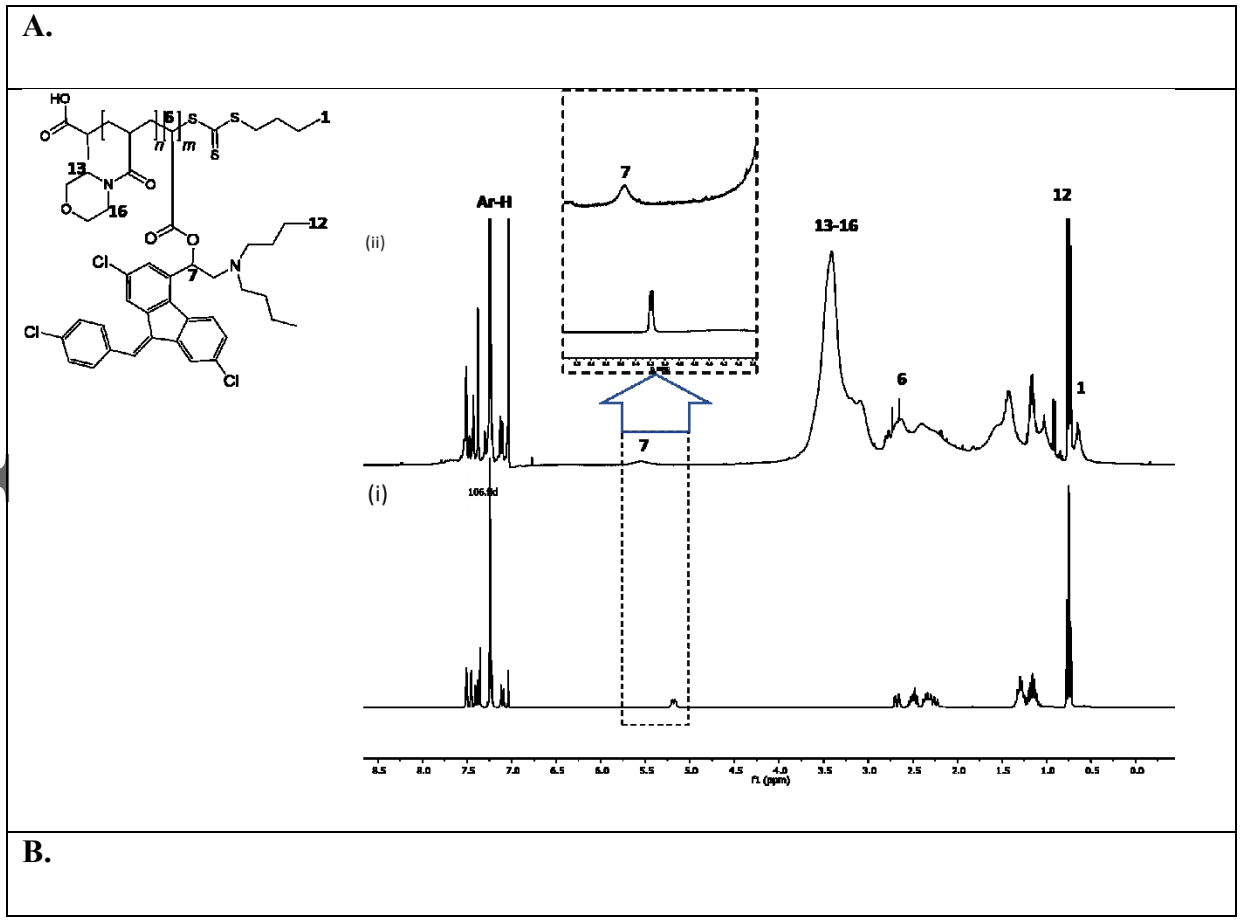

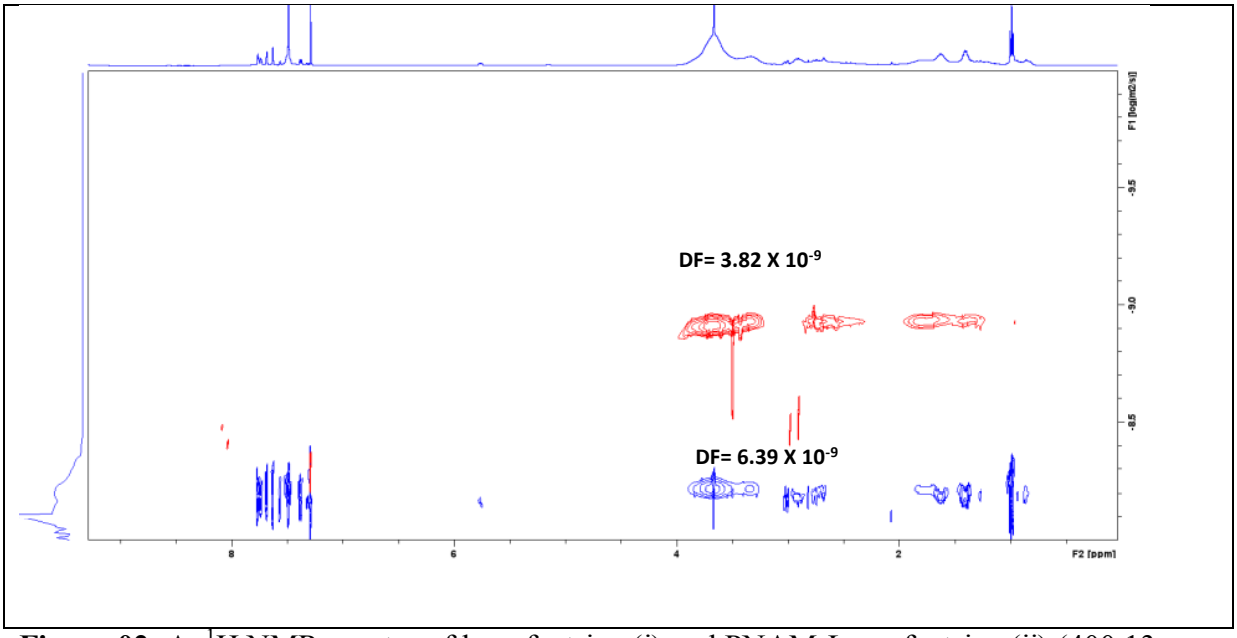

Figure 02. **A.** ^{1}H NMR spectra of lumefantrine (i) and PNAM-Lumefantrine (ii) (400.13 MHz, $CDCl_3$). Inset is the downfield shift of the oxymethine proton of lumefantrine confirming successful conjugation. Ar-H refers to the aromatic rings' hydrogens. **B.** DOSY NMR spectrum of PNAM-Lumefantrine conjugate (blue) overlayed with that of pristine PNAM (red) (500 MHz, $CDCl_3$). DOSY experiments were performed at 25 °C on a Bruker AVANCE III with a probe of type PA BBO 500 S1 BBF-H-D-05.

The conjugate had a purity of >99%, as determined by ^{1}H NMR analysis. Determination of drug loading by UV absorption spectroscopy was complicated by the absorption interference of PNAM at λ_{max} = 335 nm, which is characteristically used for the maximum absorbance of lumefantrine (28,29). The free drug content was below quantifiable limits in the last organic solvent wash of the conjugate (LLOQ = 2.0 ng/ml).

A DOSY NMR experiment confirmed the presence of the PNAM-Lumefantrine conjugate as the product of the synthesis (**Figure 02 B**). The PNAM and lumefantrine signals showed a common diffusion coefficient that was distinct from that of the original polymer.

In a controlled experiment, conjugation reactions to link the PNAM and lumefantrine were set up with and without the coupling reagent, DIC, on a parallel synthesis workstation (Radleys Carousel 12 Reaction Station). This was carried out to investigate the increase in lumefantrine solubility attributable to the polymer conjugation. After centrifugation at 21 000 *x g,* about 2450 times more lumefantrine was detectable by UV absorption spectroscopy

(LLOQ = 2 µg/ml) in the aqueous supernatant of the experiment with DIC than was detectable in the experiment where no conjugation occurred, i.e., where there was no DIC (**Figure 03**). This increase in solubility significantly improves the potential therapeutic use of lumefantrine for intravenous administration.

The conjugate exhibited hydrodynamic diameter of 91.12 ± 0.92 nm (PDI = 0.201 ± 0.01; zeta potential = -28.5 ± 1.59 mV) in dynamic light scattering analysis (**Figure 04**). The negative z-potential, probably due to unconjugated carboxylic acid groups, favours particle stability in solution by preventing aggregation.

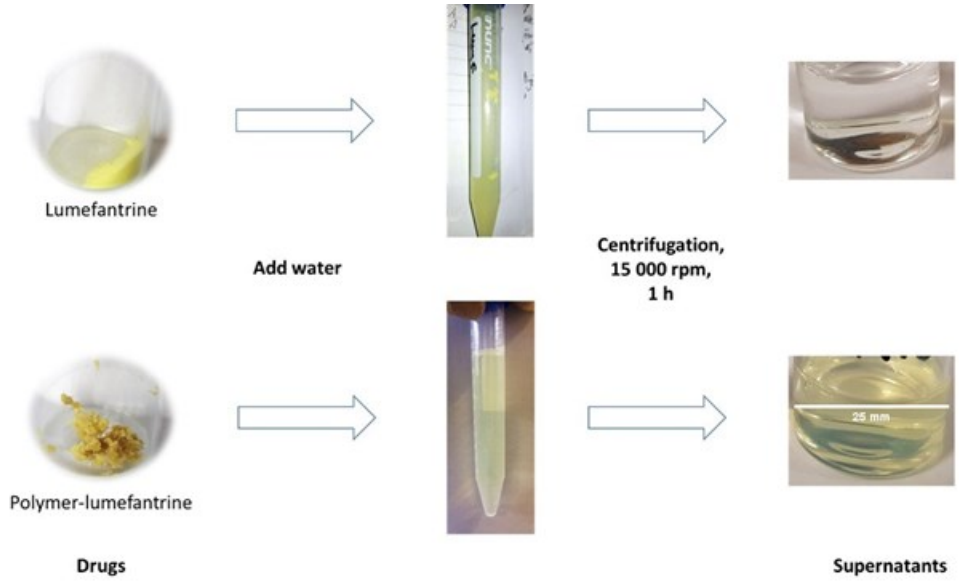

Figure 03. Demonstration of the aqueous solubility of PNAM-Lumefantrine compared to unconjugated lumefantrine through centrifugation of the respective solutions.

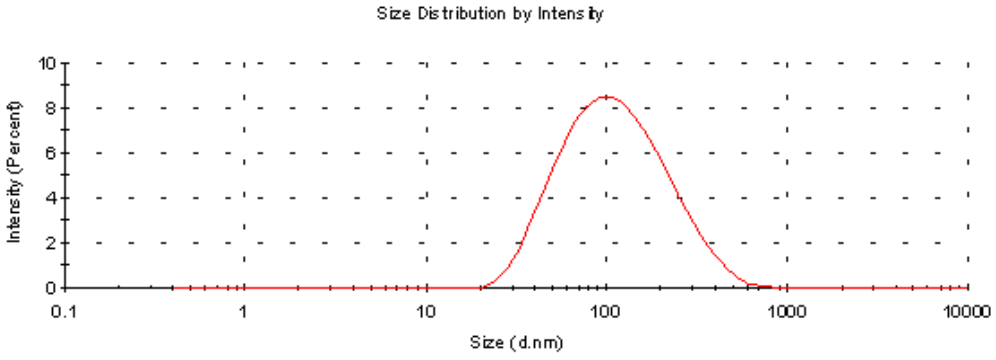

Figure 04. Average particle size distribution of PNAM-Lumefantrine conjugate.

4.2. *In vitro* antiplasmodial activity and cytotoxicity studies

Both the PNAM-Lumefantrine conjugate and the unconjugated lumefantrine showed antiplasmodial activity in SYBR Green screening assays (intraerythrocytic NF54 *P. falciparum*) at 5 µg/ml and 1.0 µg/ml drug equivalence concentrations, although the unconjugated drug demonstrated only 76 ± 10.64% (z-factor = 0.91) at the lower concentration (**Figure 05 A**). In pLDH assay, the IC_{50} of PNAM-Lumefantrine was determined to be 0.21 µg/ml (**Figure 05 B**). Lumefantrine has previously been reported to have IC_{50} ranging from 0.022 to 0.053 µg/ml for the 3D7 strain of the *P. falciparum* parasite (30). The ten-fold reduction in IC_{50} is very likely due to the prodrug nature of the conjugate and the need for the conjugate to reach the acidic food vacuole of the parasite, which requires traversing four membrane layers, for the drug to be released. The activity seen for PNAM-Lumefantrine could alternatively be due to slow hydrolysis of the polymer conjugate during the assay. PNAM-Lumefantrine and unconjugated lumefantrine were not toxic to Vero and Caco-2 cells in *in vitro* cytotoxicity assays at the maximum tested concentration (Supplementary Data **Table S3**). The free polymer did not show any significant antiplasmodial activity or cytotoxicity in any of the studies.

A.

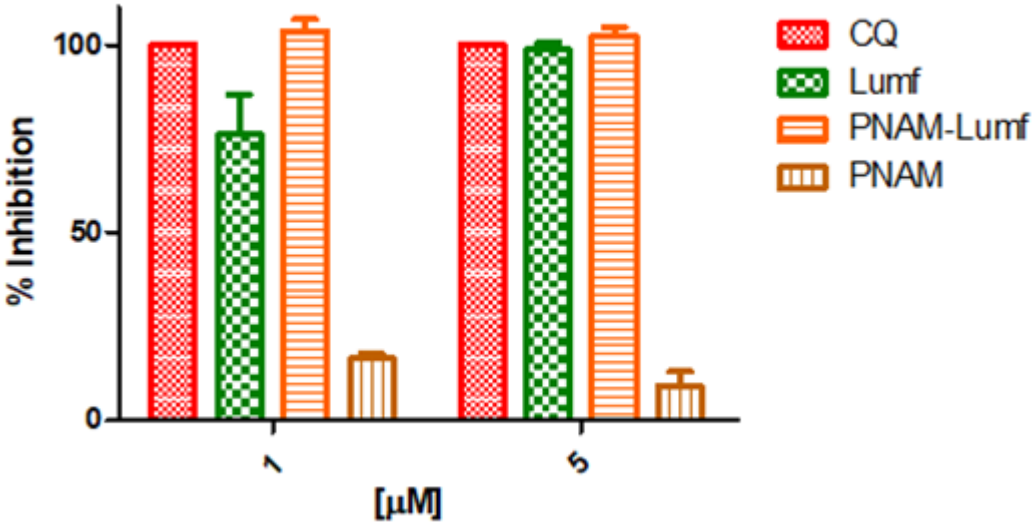

B.

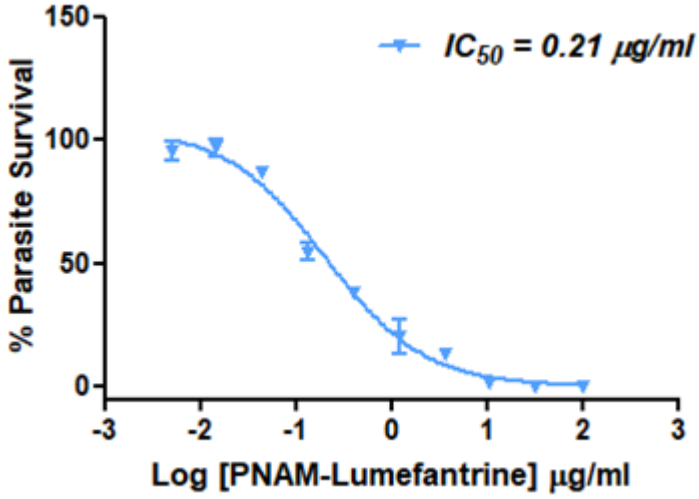

Figure 05. **A.** Antiplasmodial (NF54 *P. falciparum*) activity of PNAM-Lumefantrine conjugate at 1 µM and 5 µM concentrations. **B.** The dose-response curve used to extrapolate the 50% inhibitory concentration (IC_{50}) of PNAM-Lumefantrine tested against 3D7 *P. falciparum*. Data are expressed as mean of triplicate values ± standard deviation. [chloroquine (CQ), unconjugated lumefantrine (Lumf), PNAM-Lumefantrine (PNAM-Lumf), free polymer (PNAM)].

4.3. *In vivo* pharmacokinetics (Balb/c)

Free lumefantrine was quantifiable for up to 48 h in the plasma of mice administered PNAM-Lumefantrine and unconjugated lumefantrine (LLOQ = 4 nM) (**Figure 06**).

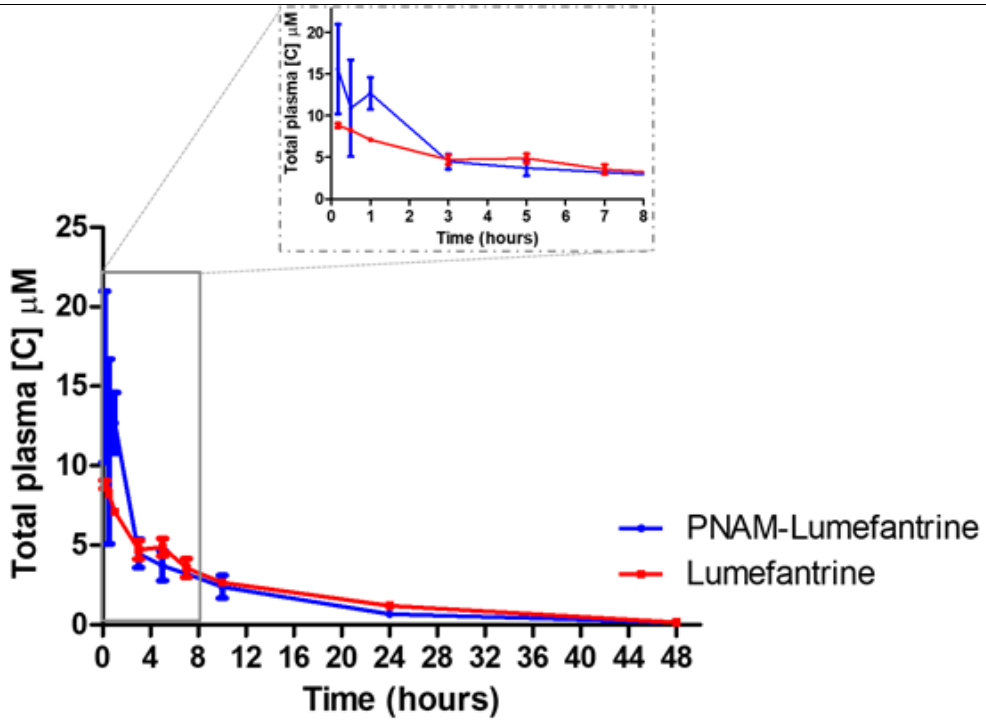

Parameter	PNAM-Lumefantrine	Reference lumefantrine
Number of animals	3	3
Nominal dose (mg/kg)	2	2
C_{max} (µM)	3.13 ± 2.56	6.11 ± 1.54
$t_{1/2}$ (h)	12.9 ± 3.5	10.3 ± 2.4
Cl (ml/min/kg)	0.73 ± 0.02	0.86 ± 0.08
Vd (l/kg)	1.9 ± 1.4	0.8 ± 0.2
Vss (l/kg)	0.45 ± 0.01	0.6 ± 0.1
$AUC_{0-\infty}$ Lumefantrine (µM.min)	5379[a] ± 143	5520[a] ± 635
$AUC_{0-\infty}$ metabolite (µM.min)	552 ± 60	ND

Figure 06. The circulating plasma concentration vs time profiles of PNAM-Lumefantrine and the unconjugated lumefantrine reference in healthy Balb/c mice. Time points represent the mean ± SEM, n = 3. ($p<0.01$)[a] No statistical difference between the values. ($p<0.01$) ND indicates that the value was not determined.

The circulating plasma concentration of lumefantrine released from the conjugate was comparable to that observed for the reference unconjugated drug with the area under the curve (AUC) of the former being 98% of the reference. Although the maximum plasma concentration (C_{max}) of the conjugate was only about half of the reference, unconjugated lumefantrine, its elimination half-life ($t_{1/2}$) was about three hours longer, indicating a time dependence for hydrolytic release of lumefantrine from the polymer.

Desbutyl-lumefantrine, a product of CYP3A4 metabolism of lumefantrine, was detectable in the plasma of the animals exposed to the PNAM-Lumefantrine conjugate (AUC = 552 ± 60 μM.min, approximately 10% of the parent) but not in the animals treated with the reference lumefantrine. In humans, the relative concentration of desbutyl-lumefantrine ranges from undetectable to about 6% (30). In rats, about 5% of desbutyl-lumefantrine has been observed relative to the parent on IV administration (31,32). On oral administration in the *P. falciparum* infected NSG mouse, about 20% of desbutyl-lumefantrine relative to parent was observed (unpublished results). Desbutyl-lumefantrine (geometric mean IC_{50} = 9.0 nM) is known to possess higher antiplasmodial activity than lumefantrine (geometric mean IC_{50} = 65.2 nM) (30). The detection of a significant amount of the liver metabolite in the plasma is a firm confirmation of uptake in this organ. It is difficult to speculate why there was no detectable quantity of desbutyl-lumefantrine in the animals treated with the unconjugated lumefantrine.

4.4. *In vivo* pharmacodynamics

At the daily dose of the lumefantrine investigated (1 mg/kg body weight), a 50% reduction in parasitaemia was observed in the animals treated with the conjugate as compared to the control animals treated with the PBS vehicle only (**Figure 07**). However, and surprisingly, there was no observable difference in the parasitaemia of the animals treated with unconjugated lumefantrine compared to those treated with the vehicle (DMA: PEG: PPG) (**Figure S5**). The reason for this was not immediately clear but may be due to a possible "encapsulation" of the drug in the polymeric components of the delivery vehicle. This could be investigated further in an experiment with varying oral lumefantrine administered to match the exposure seen with the conjugate.

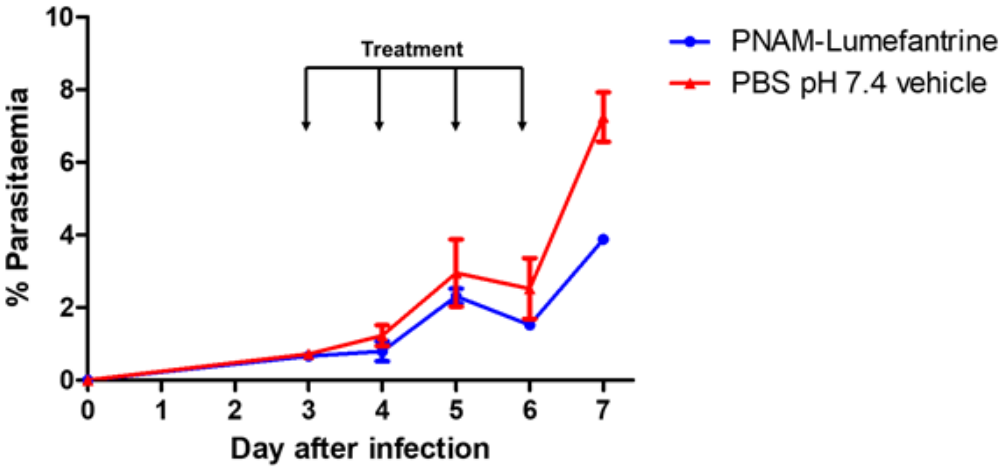

Figure 07. *In vivo* therapeutic efficacy of PNAM-Lumefantrine and the vehicle. Time points represent the mean ± SD of two *P. falciparum*-infected mice. ($p<0.01$) Limit of detection = 0.01% parasitaemia.

We investigated the pharmacokinetics for 24 h immediately after the first PNAM-Lumefantrine treatment of the infected NSG mice (Supplementary Data). During this period, the AUC of the lumefantrine was higher on administration of the drug itself than on administration of the conjugate (180 µM.min vs 161 µM.min). This was an inversion of what was observed in the healthy mice experiments, but within experimental variability. The dose normalized AUCs in the infected NSG mice were considerably lower (17-fold from administration of PNAM-Lumefantrine) than those in the uninfected Balb-c mice used for PK determinations. We assume that the use of an infected animal model, which was artificially grafted with human erythrocytes and potentially with compromised esterase capability, might have been a factor in increasing drug exposure.

5. Discussion

The low aqueous solubility of lumefantrine has precluded its development into an intravenously administered antimalarial. The recent attempt at developing a combination therapy that included a polymeric drug of lumefantrine was unsuccessful as the *in vitro* antiplasmodial activity was about a thousand times less than the combination of the free artemether and lumefantrine (11,24).

The conjugation of drug molecules to water-soluble polymeric carriers via physiologically labile linkers has been shown in cancer therapeutics to solve the problem of aqueous insolubility. Whilst drug insolubility and other pharmacological problems also exist with antimalarials, the application of this technology to malaria and many other infectious diseases has been limited (17,33). Previous applications of polymer therapeutics to infectious diseases have mostly been with antiretroviral drugs used in the treatment of HIV/AIDS (34–37). The application to malaria has mainly involved the conjugation of primaquine to a water-soluble polymer for the treatment of liver hypnozoites, a stage of the malarial parasite's life cycle that is missing in *P. falciparum* (38,39). For solubility purposes, primaquine does not require conjugation to a polymer as its bisphosphate salt is readily soluble in water. Similarly, DHA (aqueous solubility: 3.16 mg/ml) was made water-soluble for intravenous administration just by a modification to the hemisuccinate salt artesunate. We synthesized a lumefantrine-hemisuccinate conjugate that was only about 440 times more soluble than the free drug. Although the arylamino alcohol class of drugs, to which lumefantrine belongs and which also includes other antimalarials like halofantrine, mefloquine, and quinine, are generally poorly soluble in water, lumefantrine is distinguished by its extreme insolubility. Compared to other notoriously insoluble drugs like camptothecin (5.11×10^{-1} mg/ml), paclitaxel (5.56×10^{-3} mg/ml), doxorubicin (1.18 mg/ml) and amphotericin B (8.19×10^{-2} mg/ml) that have been conjugated to polymers, lumefantrine (3.09×10^{-5} mg/ml) is exceptional. Lumefantrine has therefore been a formidable challenge to make into an adequately water-soluble intravenous therapeutic.

The conjugation of lumefantrine to PNAM resulted in a significant increase in the amount of drug that could be dissolved in a volume of water although we did not investigate the maximum solubility possible. The amphipathic structure of the PNAM is believed to have both enhanced the aqueous solubility of the conjugate and aided cellular membrane penetration of the pendant drug molecules. In this scenario, lumefantrine is conjugated to the shorter hydrophobic block of the polymer while the longer hydrophilic segment extends as a solubilizing tail. With this design, the hydrophobic head would cross the plasma membrane (40). A further significance of this scenario is that it would facilitate the uptake of the conjugate into red blood cells. Red blood cells are non-endocytic, and the uptake of materials would be by passive transmembrane transport. Infected red blood cells are reported to develop new permeability pathways (NPPs) for the exchange of substances between the cell

and its environment (41). The diameter of NPPs is typically 50 to 80 nm (42,43). The PNAM-Lumefantrine conjugates were of average hydrodynamic particle size of 91.12 ± 0.92 nm, which puts a significant fraction out of range for entry via the NPPs. Direct membrane penetration facilitated by the amphiphilic structure of the conjugate is therefore a plausible contributor to activity *in vitro*. There may also be slow hydrolysis of the drug from the conjugate in culture.

The PK data of healthy mice administered the PNAM-Lumefantrine showed significant conversion of the drug to its active metabolite DBL, presumably via esterases in the blood or the liver. The relatively high plasma level of the metabolite merits further research as orally administered lumefantrine has been reported to only be converted to DBL at a very low plasma concentration (30,44). However, this is not out of line relative to what has been seen in other species (human and rat). The significance in the lumefantrine concentrations seen in the PK study is that the intravenous route results in 100% delivery of the drug to the plasma and that release from the polymer is very high. The bioavailability of lumefantrine dosed orally in patients varies considerably with considerably greater absorption associated with food intake. An intravenous delivery of the drug would give more consistent results and enable its delivery for incapacitated patients.

The 50% parasitaemia clearance achieved by the PNAM-Lumefantrine conjugate in *P. falciparum*-infected NSG mice is significant given that in oral combination treatment with artemisinin, the lumefantrine only encounters less than 5% residual parasitaemia arising from late-maturating parasites (45,46). Although recent clinical observations have indicated that the potency of the artemisinins is being challenged by increasing parasite resistance and longer clearance times, this has yet to significantly change the parasitaemia clearance burden that has to be borne by lumefantrine (47,48).

The reason for the much lower lumefantrine concentrations in the infected NSG mouse versus the Balb-c mice used in the PK determinations is not known. It is possible that esterases that are presumably responsible for release of the drug from the conjugate are compromised in the immunocompromised NSG mouse or else in the infected state.

At 48 h, the average plasma lumefantrine concentration in healthy Balb/c mice was 87.1 ± 5.6 ng/ml, down from a C_{max} 1652.64 ± 1351.68 ng/ml. In humans, a 7^{th} day plasma lumefantrine

concentration of >175 ng/ml for the orally administered drug has been reported as a putative sero-marker of a successful treatment outcome (49,50). To achieve and sustain a high circulating lumefantrine level may require a more branched polymer architecture. Branched chains, dendrimeric, or star polymers have been shown to circulate for extended periods (51–53).

Artesunate is currently administered orally in three of the five WHO-approved ACTs while its synthetic precursor and hepatic metabolite, DHA, is in a fourth ACT (4). It is therefore absent only in the artemether-lumefantrine (AL) combination. Notably artesunate has sufficiently high solubility to enable IV administration. Both artemether and artesunate share DHA as a common metabolite. Given this compatibility of artesunate with a wide variety of other antimalarials and its use as the first treatment step in severe malaria—followed immediately by the full oral course of AL—we believe that a new intravenous combination with a water-soluble lumefantrine as developed here will be safe and well tolerated. Lumefantrine has been demonstrated to improve the parasitaemia clearance activity of artemisinins during the critical resistance window when parasite susceptibility is sub-optimum (10). This is the early ring stage period that may allow the parasite to survive the brief plasma half-life of the artemisinins.

6. Conclusion

In this study, we reported on the development and demonstration of a new antimalarial therapeutic that represents the first intravenous administration of a truly water-soluble lumefantrine made by conjugation to a carrier polymer via a physiologically labile ester linker. We used a new block co-polymer, PNAM, with a short multivalent hydrophobic block and a long non-conjugating hydrophilic block. With this amphiphilic architecture, we were able to significantly increase the aqueous solubility of lumefantrine that allowed for a safe intravenous administration in mice. After administration to healthy mice, the PK showed rapid release of lumefantrine with a notable production of the liver metabolite desbutyl-lumefantrine. This is considered very promising for the therapeutic given that red blood cells are non-endocytic, and the particle size range of the conjugate is likely too large for entry. Following PNAM-Lumefantrine treatment of *P. falciparum*-infected NSG mice, we observed a 50% reduction in total parasitaemia as compared to animals treated with unconjugated

lumefantrine. We believe that with further development, a polymer-based lumefantrine therapeutic can be formulated with an artemisinin (for example artesunate) into a powerful combination therapy for a simple single-course treatment of severe malaria.

7. Abbreviations

LLOQ	lower limit of quantification
LC-MS/MS	Liquid Chromatography with tandem mass spectrometry
LC_{50}	50% Lethal Concentration

8. Author contributions

M.O.B. developed the concept and design of the project. A.S.C. was the project administrator. Synthesis and physico-chemical characterization steps were performed by W.M.R.M., S.M., L.L.T. and Z.E.D.C. Cell assays were performed by W.M.R.M, I.M.F. and L.J.M. In vivo experiments were performed by D.T., L.G., and G.S.B. All authors were involved in the analysis and interpretation of the data. The manuscript was written by W.M.R.M. and M.O.B. and revised by L.A.P., G.S.B., and M.O.B. All authors have given approval for the final version of the manuscript.

9. Declaration of competing interest

All authors declare no competing or conflicting interests.

10. Acknowledgements

The authors acknowledge the support of the World Health Organization and the South African Medical Research Council through the CEWG Demonstration project grant and the National Research Foundation of South Africa (grant numbers: 104907 and 114369) for financial support. The University of Pretoria provided postdoctoral funding to I.M.F. The

authors acknowledge and express gratitude to Dr Mamoalosi Selepe for the DOSY NMR experiments.

11. Appendix A. Supplementary data

More materials, methods, physico-chemical characterization and biological assay protocols, supplementary figures, and tables can be found in the Electronic Supplementary Data.

12. References

1. World Health Organization. WorldMalariaReport-2021 [Internet]. 2021 [cited 2022 Jun 1]. Available from: https://www.who.int/publications/i/item/9789240040496

2. Wassmer SC, Grau GER. Severe malaria: what's new on the pathogenesis front? Vol. 47, International Journal for Parasitology. Elsevier Ltd; 2017. p. 145–52.

3. Wassmer SC, Taylor TE, Rathod PK, Mishra SK, Mohanty S, Arevalo-Herrera M, et al. Investigating the pathogenesis of severe malaria: A multidisciplinary and cross-geographical approach. American Journal of Tropical Medicine and Hygiene. 2015;93(Suppl 3):42–56.

4. World Health Organization. Guidelines for the treatment of malaria. 2015.

5. Bosman A, Mendis KN. A major transition in malaria treatment: The adoption and deployment of artemisinin-based combination therapies. American Journal of Tropical Medicine and Hygiene. 2007;77(SUPPL. 6):193–7.

6. Minzi O, Maige S, Sasi P, Ngasala B. Adherence to artemether-lumefantrine drug combination: A rural community experience six years after change of malaria treatment policy in Tanzania. Malaria Journal. 2014 Jul 10;13(1):267.

7. Ashley EA, Stepniewska K, Lindegårdh N, McGready R, Annerberg A, Hutagalung R, et al. Pharmacokinetic study of artemether-lumefantrine given once daily for the treatment of uncomplicated multidrug-resistant falciparum malaria. Tropical Medicine and International Health. 2007 Feb;12(2):201–8.

8. Uwimana A, Umulisa N, Venkatesan M, Svigel SS, Zhou Z, Munyaneza T, et al. Association of Plasmodium falciparum kelch13 R561H genotypes with delayed parasite clearance in Rwanda: an open-label, single-arm, multicentre, therapeutic efficacy study. The Lancet Infectious Diseases. 2021 Aug 1;21(8):1120–8.

9. Balikagala B, Fukuda N, Ikeda M, Katuro OT, Tachibana SI, Yamauchi M, et al. Evidence of Artemisinin-Resistant Malaria in Africa. New England Journal of Medicine. 2021 Sep 23;385(13):1163–71.

10. Kümpornsin K, Loesbanluechai D, de Cozar C, Kotanan N, Chotivanich K, White NJ, et al. Lumefantrine attenuates Plasmodium falciparum artemisinin resistance during the early ring stage. International Journal for Parasitology: Drugs and Drug Resistance [Internet]. 2021;17(September):186–90. Available from: https://doi.org/10.1016/j.ijpddr.2021.09.005

11. Prabhu P, Suryavanshi S, Pathak S, Patra A, Sharma S, Patravale V. Nanostructured lipid carriers of artemether–lumefantrine combination for intravenous therapy of cerebral malaria. International Journal of Pharmaceutics. 2016;513(1–2):504–17.

12. Pink DL, Loruthai O, Ziolek RM, Wasutrasawat P, Terry AE, Lawrence MJ, et al. On the Structure of Solid Lipid Nanoparticles. Small. 2019 Nov 1;15(45).

13. Yoo JW, Chambers E, Mitragotri S. Factors that Control the Circulation Time of Nanoparticles in Blood: Challenges, Solutions and Future Prospects. Current Pharmaceutical Design [Internet]. 2010 Jul 1 [cited 2022 Jun 1];16(21):2298–307. Available from: http://www.eurekaselect.com/openurl/content.php?genre=article&issn=1381-6128&volume=16&issue=21&spage=2298

14. Lball R, Bajaj P, Whitehead KA. Achieving long-term stability of lipid nanoparticles: Examining the effect of pH, temperature, and lyophilization. International Journal of Nanomedicine. 2017;12:305–15.

15. Schoenmaker L, Witzigmann D, Kulkarni JA, Verbeke R, Kersten G, Jiskoot W, et al. mRNA-lipid nanoparticle COVID-19 vaccines: Structure and stability. Vol. 601, International Journal of Pharmaceutics. Elsevier B.V.; 2021. p. 120586.

16. Qian C, Decker EA, Xiao H, McClements DJ. Impact of lipid nanoparticle physical state on particle aggregation and β-carotene degradation: Potential limitations of solid lipid nanoparticles. Food Research International. 2013 Jun 1;52(1):342–9.

17. Mvango S, Matshe WMR, Balogun AO, Pilcher LA, Balogun MO. Nanomedicines for Malaria Chemotherapy: Encapsulation vs. Polymer Therapeutics [Internet]. Vol. 35, Pharmaceutical Research. Pharmaceutical Research; 2018. p. 237. Available from: http://link.springer.com/10.1007/s11095-018-2517-z

18. Pang X, Jiang Y, Xiao Q, Leung AW, Hua H, Xu C. pH-responsive polymer–drug conjugates: Design and progress. Journal of Controlled Release [Internet]. 2016 Jan 28 [cited 2018 Jun 21];222:116–29. Available from: https://www.sciencedirect.com/science/article/pii/S0168365915302765?via%3Dihub

19. Schluep T, Cheng J, Khin KT, Davis ME. Pharmacokinetics and biodistribution of the camptothecin-polymer conjugate IT-101 in rats and tumor-bearing mice. Cancer Chemotherapy and Pharmacology. 2006;57(5):654–62.

20. Chipman SD, Oldham FB, Pezzoni G, Singer JW. Biological and clinical characterization of paclitaxel poliglumex (PPX, CT-2103), a macromolecular polymer-drug conjugate. Vol. 1, International Journal of Nanomedicine. 2006. p. 375–83.

21. Liang L, Lin SW, Dai W, Lu JK, Yang TY, Xiang Y, et al. Novel cathepsin B-sensitive paclitaxel conjugate: Higher water solubility, better efficacy and lower toxicity. Journal of Controlled Release. 2012 Jun 28;160(3):618–29.

22. Dai L, Wang L, Deng L, Liu J, Lei J, Li D, et al. Novel multiarm polyethylene glycol-dihydroartemisinin conjugates enhancing therapeutic efficacy in non-small-cell lung cancer. Scientific Reports. 2014;4(5871).

23. Alven S, Aderibigbe BA, Balogun MO, Matshe WMR, Ray SS. Polymer-drug conjugates containing antimalarial drugs and antibiotics. Journal of Drug Delivery Science and Technology [Internet]. 2019; 53:101171. Available from: https://doi.org/10.1016/j.jddst.2019.101171

24. Fortuin L, Leshabane M, Pfukwa R, Coertzen D, Birkholtz L marie, Klumperman B. Facile Route to Targeted, Biodegradable Polymeric Prodrugs for the Delivery of Combination Therapy for Malaria. ACS Biomater Sci Eng. 2020;6(11).

25. Makler MT, Hinrichs DJ. Measurement of the lactate dehydrogenase activity of Plasmodium falciparum as an assessment of parasitemia. American Journal of Tropical Medicine and Hygiene. 1993 Feb 1;48(2):205–10.

26. Verlinden BK, Niemand J, Snyman J, Sharma SK, Beattie RJ, Woster PM, et al. Discovery of novel alkylated (bis)urea and (bis)thiourea polyamine analogues with potent antimalarial activities. Journal of Medicinal Chemistry. 2011 Oct 13;54(19):6624–33.

27. Angulo-Barturen I, Jiménez-Díaz MB, Mulet T, Rullas J, Herreros E, Ferrer S, et al. A murine model of falciparum-malaria by in vivo selection of competent strains in non-myelodepleted mice engrafted with human erythrocytes. PLoS ONE. 2008 May 21;3(5).

28. Mansor SM, Navaratnam V, Yahaya N, Nair NK, Wernsdorfer WH, Degen PH. Determination of a new antimalarial drug, benflumetol, in blood plasma by high-performance liquid chromatography. Journal of Chromatography B. 1996;6(2):1–1.

29. Ezzet F, Mull R, Karbwang J. Population pharmacokinetics and therapeutic response of CGP 56697 (artemether + benflumetol) in malaria patients. British Journal of Clinical Pharmacology. 1998;46(6):553–61.

30. Wong RPM, Salman S, Ilett KF, Siba PM, Mueller I, Davis TME. Desbutyl-lumefantrine is a metabolite of lumefantrine with potent in vitro antimalarial activity that may influence

artemether-lumefantrine treatment outcome. Antimicrobial Agents and Chemotherapy. 2011;55(3):1194–8.

31. Wahajuddin, Singh SP, Jain GK. Gender differences in pharmacokinetics of lumefantrine and its metabolite desbutyl-lumefantrine in rats. Biopharmaceutics and Drug Disposition. 2012 May;33(4):229–34.

32. Wahajuddin, Singh SP, Raju KSR, Nafis A, Puri SK, Jain GK. Intravenous pharmacokinetics, oral bioavailability, dose proportionality and in situ permeability of anti-malarial lumefantrine in rats. Malaria Journal. 2011;10.

33. Neves Borgheti-Cardoso L, San Anselmo M, Lantero E, Lancelot A, Serrano JL, Hernández-Ainsa S, et al. Promising nanomaterials in the fight against malaria. Journal of Materials Chemistry B. 2020 Nov 7;8(41):9428–48.

34. Gunaseelan S, Debrah O, Wan L, Leibowitz MJ, Rabson AB, Stein S, et al. Synthesis of poly(ethylene glycol)-based saquinavir prodrug conjugates and assessment of release and anti-HIV-1 bioactivity using a novel protease inhibition assay. Bioconjugate Chemistry. 2004;15(6):1322–33.

35. Danial M, Telwatte S, Tyssen D, Cosson S, Tachedjian G, Moad G, et al. Combination anti-HIV therapy via tandem release of prodrugs from macromolecular carriers. Polym Chem. 2016;7(48):7477–87.

36. Wannachaiyasit S, Chanvorachote P, Nimmannit U. A Novel Anti-HIV Dextrin–Zidovudine Conjugate Improving the Pharmacokinetics of Zidovudine in Rats. AAPS PharmSciTech [Internet]. 2008;9(3):840–50. Available from: http://www.springerlink.com/index/10.1208/s12249-008-9122-0

37. Li W, Wu J, Zhan P, Chang Y, Pannecouque C, de Clercq E, et al. Synthesis, drug release and anti-HIV activity of a series of PEGylated zidovudine conjugates. International Journal of Biological Macromolecules. 2012 May 1;50(4):974–80.

38. Tomiya N, Jardim JG, Hou J, Pastrana-Mena R, Dinglasan RR, Lee YC. Liver-targeting of primaquine-(poly-γ-glutamic acid) and its degradation in rat hepatocytes. Bioorganic and Medicinal Chemistry. 2013;21(17):5275–81.

39. Srinivasan S, Roy D, Chavas TEJ, Vlaskin V, Ho DK, Pottenger A, et al. Liver-targeted polymeric prodrugs of 8-aminoquinolines for malaria radical cure. Journal of Controlled Release. 2021 Mar 10;331:213–27.

40. Paloncýová M, Devane R, Murch B, Berka K, Otyepka M. Amphiphilic drug-like molecules accumulate in a membrane below the head group region. Journal of Physical Chemistry B. 2014 Jan 30;118(4):1030–9.

41. Bouyer G, Barbieri D, Dupuy F, Marteau A, Sissoko A, N'Dri ME, et al. Plasmodium falciparum sexual parasites regulate infected erythrocyte permeability. Communications Biology. 2020 Dec 1;3(1).

42. Patra S, Singh M, Wasnik K, Pareek D, Gupta PS, Mukherjee S, et al. Polymeric Nanoparticle Based Diagnosis and Nanomedicine for Treatment and Development of Vaccines for Cerebral Malaria: A Review on Recent Advancement. Vol. 4, ACS Applied Bio Materials. American Chemical Society; 2021. p. 7342–65.

43. Anamika J, Nikhar V, Laxmikant G, Priya S, Sonal V, Vyas SP. Nanobiotechnological modules as molecular target tracker for the treatment and prevention of malaria: options and opportunity. Drug Delivery and Translational Research. 2020 Aug 1;10(4):1095–110.

44. Noedl H, Allmendinger T, Prajakwong S, Wernsdorfer G, Wernsdorfer WH. Desbutyl-benflumetol, a novel antimalarial compound: In vitro activity in fresh isolates of Plasmodium falciparum from Thailand. Antimicrobial Agents and Chemotherapy. 2001;45(7):2106–9.

45. van Vugt M, Looareesuwan S, Wilairatana P, McGready R, Villegas L, Gathmann I, et al. Artemether-lumefantrine for the treatment of multidrug-resistant falciparum malaria. Trans R Soc Trop Med Hyg. 2000;94(5):545–8.

46. White NJ, van Vugt M, Ezzet F. Clinical pharmacokinetics and pharmacodynamics of artemether-lumefantrine. Vol. 37, Clinical Pharmacokinetics. Adis International Ltd; 1999. p. 105–25.

47. Ashley EA, Dhorda M, Fairhurst RM, Amaratunga C, Lim P, Suon S, et al. Spread of Artemisinin Resistance in Plasmodium falciparum Malaria. New England Journal of Medicine. 2014;371(5):411–23.

48. Wang J, Xu C, Lun ZR, Meshnick SR. Unpacking 'Artemisinin Resistance.' Vol. 38, Trends in Pharmacological Sciences. Elsevier Ltd; 2017. p. 506–11.

49. Price RN, Uhlemann AC, van Vugt M, Brockman A, Hutagalung R, Nair S, et al. Molecular and Pharmacological Determinants of the Therapeutic Response to Artemether-Lumefantrine in Multidrug-Resistant Plasmodium falciparum Malaria. Clinical Infectious Diseases. 2006;42(11):1570–7.

50. Artemether-lumefantrine treatment of uncomplicated Plasmodium falciparum malaria: a systematic review and meta-analysis of day 7 lumefantrine concentrations and therapeutic response using individual patient data. BMC Med. 2015 Sep 18;13:227.

51. Duro-Castano A, Movellan J, Vicent MJ. Smart branched polymer drug conjugates as nano-sized drug delivery systems. Biomaterials Science. 2015 Oct 1;3(10):1321–34.

52. Prencipe G, Tabakman SM, Welsher K, Liu Z, Goodwin AP, Zhang L, et al. PEG branched polymer for functionalization of nanomaterials with ultralong blood circulation. J Am Chem Soc. 2009 Apr 8;131(13):4783–7.

53. Etrych T, Šubr V, Strohalm J, Šírová M, Říhová B, Ulbrich K. HPMA copolymer-doxorubicin conjugates: The effects of molecular weight and architecture on biodistribution and in vivo activity. In: Journal of Controlled Release. 2012. p. 346–54.